Eur. Phys. J. B **42**, 3–10 (2004)
DOI: 10.1140/epjb/e2004-00352-1

THE EUROPEAN PHYSICAL JOURNAL B

# Critical vortex line length near a zigzag of pinning centers

A.R. de C. Romaguera[a] and M.M. Doria[b]

Instituto de Física, Universidade Federal do Rio de Janeiro, C. P. 68528 CEP 21941-972, Rio de Janeiro, RJ, Brazil

Received 14 April 2004 / Received in final form 23 July 2004
Published online 26 November 2004 

**Abstract.** A vortex line passes through as many pinning centers as possible on its way from one extremety of the superconductor to the other at the expense of increasing its self-energy. In the framework of the Ginzburg-Landau theory we study the relative growth in length, with respect to the straight line, of a vortex near a zigzag of defects. The defects are insulating pinning spheres that form a three-dimensional cubic array embedded in the superconductor. We determine the depinning transition beyond which the vortex line no longer follows the critical zigzag path of defects.

**PACS.** 74.80.-g Spatially inhomogeneous structures – 74.25.-q General properties; correlations between physical properties in normal and superconducting states – 74.20.De Phenomenological theories (two-fluid, Ginzburg-Landau, etc.)

## 1 Introduction

The magnetic field penetrates the superconductor in the form of filaments that pierce the sample from one extremety to the other. The filament is a vortex line carrying a quantized unit of magnetic flux, $\Phi_0 = hc/2e$, where in its core the magnetic field reaches its maximum value inside the superconductor. The vortex line is not rigid and many factors can contribute to its length such as thermal fluctuations, the geometry of the sample, anisotropy, and most important of all, imperfections inside the superconductor, specially pinning centers. At the center of a flat sample, for instance, with the applied magnetic field perpendicular to the main surface, the length of the vortex line is the height of the sample. However the vortex line will tend to adjust its length to the distribution of pinning centers so to pass through as many of them as possible resulting in a vortex line bigger than the height of the sample. The nucleation of a vortex line on a pinning center is advantageous [1] for the superconductor because both the core of the vortex line and the pinning center are non-superconducting regions. Nevertheless long detours optimize the number of pinning centers visited by the vortex to a maximum, but this makes the vortex line too long and this increases its self-energy, which grows with its length.

The study of pinning centers is fundamental to the understanding of superconductors [2]. The interaction of pinning centers with vortices has been studied using several approaches [2,3]. Superconducting samples are plagued with natural pinning centers and a way to attack the problem is to consider samples with artificially made pinning centers [4], such as columnar defects [5,6], antidots [7,8] and micro holes [9]. They are interesting because they bring clear-cut questions about the interaction between vortices and pinning centers, such as the one we are interested here concerning the local misalignment of a vortex line. A vortex line is aligned to the magnetic induction direction in the absence of pinning centers, but in presence of them bends and acquires a new shape, though it remains globally oriented along the magnetic induction.

In the classical problem of the travelling salesman [10] the seller must find the shortest route that connects several cities at well known locations that he must visit. This is a minimization problem that in case of a large number of cities has many local minima, that is, many possible routes very close in length to the shortest one. Similarly to the travelling salesman, one may wonder what is the maximum length that a vortex line can reach inside a superconductor with pinning centers. To study the relative maximum length we consider the vortex line near a zigzag of pinning centers, namely, a path with abrupt alternate right and left turns such that at each turn there is a pinning center. The pinning centers are just of one kind, insulating spheres of radius $R$. Figures 1 and 2 give a pictorial view of this superconductor with pinning centers. The vortex line acquires this zigzag shape as long as trapping by the pinning centers is advantageous as compared to the increase in length caused by the zigzag path.

[a] e-mail: ton@if.ufrj.br
[b] e-mail: mmd@if.ufrj.br

There is a critical path that sets a depinning transition beyond which the vortex line does not follow the zigzag path of the pinning centers. Here we numerically determine this transition without considering thermal fluctuations. We treat the problem in the framework of the Ginzburg-Landau theory [11]. From the point of view of the Ginzburg-Landau theory, pinning may be caused by spatial fluctuations of the critical temperature, $T_c(\boldsymbol{x})$ [12], or of the mean free-path that changes the coefficient in front of the gradient term, $\xi(\boldsymbol{x})^2|(\boldsymbol{\nabla} - \frac{2\pi i}{\Phi_0}\boldsymbol{A})\Delta|^2$. The interaction between a vortex line and a pinning center has been considered by many authors in the context of the Ginzburg-Landau theory [13–16].

The paper is organized as follows. In Section 2 we describe the present model of a superconductor with pinning centers, and in Section 3 our theoretical approach is discussed. In Section 4 we give our results obtained through numerical simulations. In Section 5 we summarize the main achievements of this work.

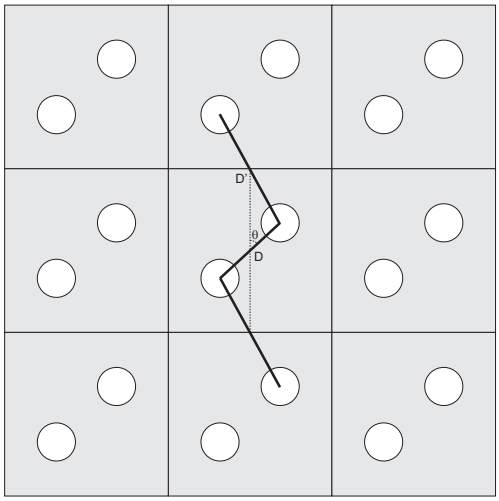


**Fig. 2.** Pictorial view of several unit cells forming the pinning center lattice.

## 2 Model

The model consists of a superconductor with a cubic array of defects, described by its simplest unit cell, a cube of size $L$ containing two pinning spheres inside, separated by $D$, as shown in Figure 1. The geometric center of these two pinning spheres coincides with the center of the unit cell. The general pinning center distribution is obtained by rotating the center of the segment $D$ by an angle $\theta$ with respect to the axis along which is oriented the magnetic induction, hereafter called $z$-axis, on a fixed plane defined by both $x$- and $z$-axes. The magnetic flux that crosses the face perpendicular to the $z$-axis of the unit cell is $\Phi_0$ and each vortex line is near a zigzag of pinning spheres, made by the pile of unit cells along the $z$-axis, according to Figure 2.

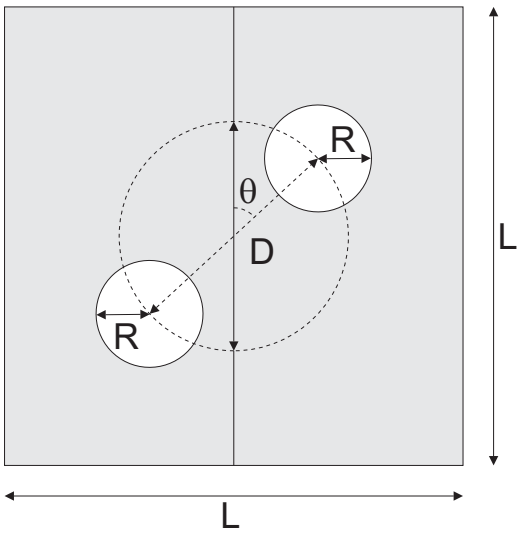


**Fig. 1.** Position of the defects inside the unit cell. The superconducting material occupies the filled region.

Though the present model treats a vortex lattice, the depinning transition is that of a single isolated vortex line near the zigzag of defects. The vortex-vortex interaction has no effect on this transition since the vortex-defect interaction is short ranged and very strong. In this paper we obtain the depinning transition for the cubic lattice of defects with $L = 12.0\xi$, $D = 6.0\xi$, and several pinning sphere radii are considered, ranging from $R = 1.2\xi$ to the maximum possible radius, $3.0\xi$, with an increment of $0.20\xi$.

To understand the length of the vortex line in this model, first consider $\theta = 0°$, where the zigzag collapses into a straight line made of two alternate segments, $D$ and $L - D$. Thus the maximum pinning sphere that fits this unit cell has radius equal to $(L - D)/2$. For arbitrary $\theta$, the segment connecting the top (bottom) pinning center to the nearest neighbor pinning center in the unit cell above (below), is $D' = \sqrt{(L-D)^2 + 4LD\sin^2(\theta/2)}$. Notice that the pinning center density is $\theta$ independent, and equal to $2/L^3$. The depinning transition is described either by the critical angle $\theta_c$, or by the relative pinning length, $\Delta l/l\big|_c = [l(\theta_c) - l(0°)]/l(0°)$, $l(\theta_c)$ being the critical length of the zig-zag path and $l(0°)$ the length of the straight line formed by alternate $D$ and $D'$ segments along the $z$-axis. From geometry one obtains that,

$$\frac{\Delta l}{l}(\theta) = \frac{\sqrt{(L-D)^2 + 4DL\sin^2(\theta/2)} - (L-D)}{L}. \quad (1)$$

It is more interesting to characterize the depinning transition through the relative pinning length $\Delta l/l$ because it also describes, though approximately, the relative length growth of the vortex line due to the presence of the zigzag of pinning centers. The maximum zigzag path possible, and consequently, the maximum length that the vortex line can achieve, occurs for $\theta = 90°$. Thus for the present set of parameters the maximum relative growth of the

vortex line possible is $(\Delta l/l)_{max} = (\sqrt{5}-1)/2$, that is the line can be $61,8\%$ bigger than a straight line, as found from equation (1).

## 3 Theoretical approach

The numerical search for the free energy minima is carried for the unit cell with the two pinning spheres inside, taking care that the well-known Saint-James de Gennes [17] boundary condition is satisfied at their surfaces because they are insulating spheres. The radial component of the supercurrent must vanish there. The unit cell has quasi-periodic boundary conditions so to describe a cubic array of pinning spheres embedded in the superconductor. This system is studied here using a Ginzburg-Landau free energy expansion that considers superconducting and non-superconducting regions on equal footing and enforces this boundary condition during the minimization procedure.

Notice that the choice of the simplest unit cell helps the minimization concerning the computational time, but from the other side forbids the onset of vortex line configurations other than the zigzag one. More complex vortex configurations in that cubic lattice of pinning centers require a larger unit cell to be studied. The present numerical procedure uses a mesh of $P^3$ points to describe the unit cell, and for the present simulations we take that $P = 19$. Thus the distance between two consecutive mesh points is $a = 2\xi/3$, and one obtains that $L = 2\xi(P-1)/3$. The local field $\boldsymbol{h} = \nabla \times \boldsymbol{A}$ is constant inside the unit cell and equal to the magnetic induction, $\boldsymbol{B}$. The regime treated here is of strong type-II superconductors with the London penetration length much larger than the unit cell ($\lambda \gg \ L > \xi$). The free energy depends on $P^3$ times the number of variables, and in our case, just the variables $Re(\Delta)$ and $Im(\Delta)$ participate in the minimization procedure. Under this considerations, we numerically minimized $2P^3$ variables through the Simulated Annealing method, a Monte Carlo thermal procedure. We take 1600 visits per site for each Monte Carlo temperature, with 150 temperature reductions, though this last number depends on how fast convergence to the absolute minimum is achieved.

To obtain the vortex solution in presence of the two pinning spheres, we minimize the Ginzburg-Landau free energy inside the unit cell assuming that the magnetic flux that crosses the cube along $z$ perpendicular faces is $\Phi_0$, and this corresponds to a magnetic induction $\boldsymbol{B} = 2\pi\kappa(\xi/L)^2\hat{z}$, in units $\sqrt{2}H_c$, where $\kappa$ is the Ginzburg-Landau constant and $H_c$ is the superconductor critical field. Under this condition a single vortex nucleates inside the unit cell. In a coordinate system whose origin is at the center of the unit cell, and the axis are along the cube's main directions, the positions of the pinning spheres, are $\boldsymbol{x}_1 = R(\sin\theta\hat{x} + \cos\theta\hat{z})$, and $\boldsymbol{x}_2 = -\boldsymbol{x}_1$, as specified in Figure 1. In this approach the pinning centers are described by step-like functions, zero inside and one outside, which are made smooth for numerical reasons, $\tau(\boldsymbol{x}) = \tau_1(\boldsymbol{x})\tau_2(\boldsymbol{x})$, $\tau_i(\boldsymbol{x}) = 1 - 2/\{\ 1 + \exp\left[(|\boldsymbol{x} - \boldsymbol{x}_i|/R)^K\right]\ \}$, with $K = 8$, $i = 1, 2$. The free energy density is,

$$\mathcal{F} = \int \frac{dv}{V}\Bigg\{ \tau(\boldsymbol{x}) \left[\xi^2 \left| \left(\boldsymbol{\nabla} - \frac{2\pi i}{\Phi_0}\boldsymbol{A}\right)\Delta\right|^2 - |\Delta|^2\right] + \frac{1}{2}|\Delta|^4\Bigg\}, \quad (2)$$

expressed in units of the critical field energy density, $H_c^2/4\pi$, and the superconducting density $|\Delta|^2$ normalized between zero and one. This free energy density takes value in the range 0 and –0.5, its minimum and maximum, respectively. These extremes correspond to the normal and the spatially constant superconducting density states, respectively. The constant density state differs from the normal state by a constant, equal to the condensation energy $H_c^2/8\pi$. The magnetic energy density also yields a constant taken to vanish for each value of the magnetic induction. Because $\tau = 0$ inside the spheres, equation (2) has the trivial solution $\Delta = 0$ with the condition $\hat{n}\cdot(\boldsymbol{\nabla} - \frac{2\pi i}{\Phi_0}\boldsymbol{A})\Delta\Big|_{surface} = 0$ satisfied at the pinning spheres surfaces.

To gain some insight into the free energy expansion of equation (2), we look at the contribution that an empty pinning sphere brings to the free energy in case of no vortices in the unit cell. A defect-free superconductor reaches the maximum density everywhere, $|\Delta|^2 = 1$, and its free energy density is simply $\mathcal{F}_0 = -0.5$, according to equation (2). The superconductor with the two pinning centers per unit cell has a higher energy because inside the pinning centers the order parameter should vanish, $|\Delta|^2 = 0$, rendering its free energy density approximately equal to the defect-free case removed of the volume of the two spheres [18], thus equal to $\mathcal{F}_0(1 - 8\pi R^3/3L^3)$. This result is only approximately valid since the curvature of the order parameter near the pinning sphere surface causes an increase in the kinetic energy, an effect that becomes more pronounced for large spheres. The kinetic energy density,

$$\mathcal{F}_{kin} = \int \frac{dv}{V}\,\tau\,\xi^2 \left| \left(\boldsymbol{\nabla} - \frac{2\pi i}{\Phi_0}\boldsymbol{A}\right)\Delta\right|^2, \quad (3)$$

is more sensitive to the depinning transition [19] than the total free energy density. The term $\boldsymbol{\nabla}\Delta$ picks a large contribution when the vortex detaches from a pinning sphere because the order parameter must bend at an extra superconductor-insulator interface.

## 4 Results

The free energy density versus $R$ is shown in Figure 3a from 0° to 90°, in steps of 9°. To understand the growth of the free energy with respect to $R$, firstly consider, the $\theta = 0°$ curve, the lowest one in free energy. The vortex line is pinned to the two aligned spheres along the $z$-axis. Considering the vortex core as a non-superconducting cylinder of radius $\xi$, it follows that for $R \leq \xi$ the two pinning spheres are fully inside the vortex core, but not for

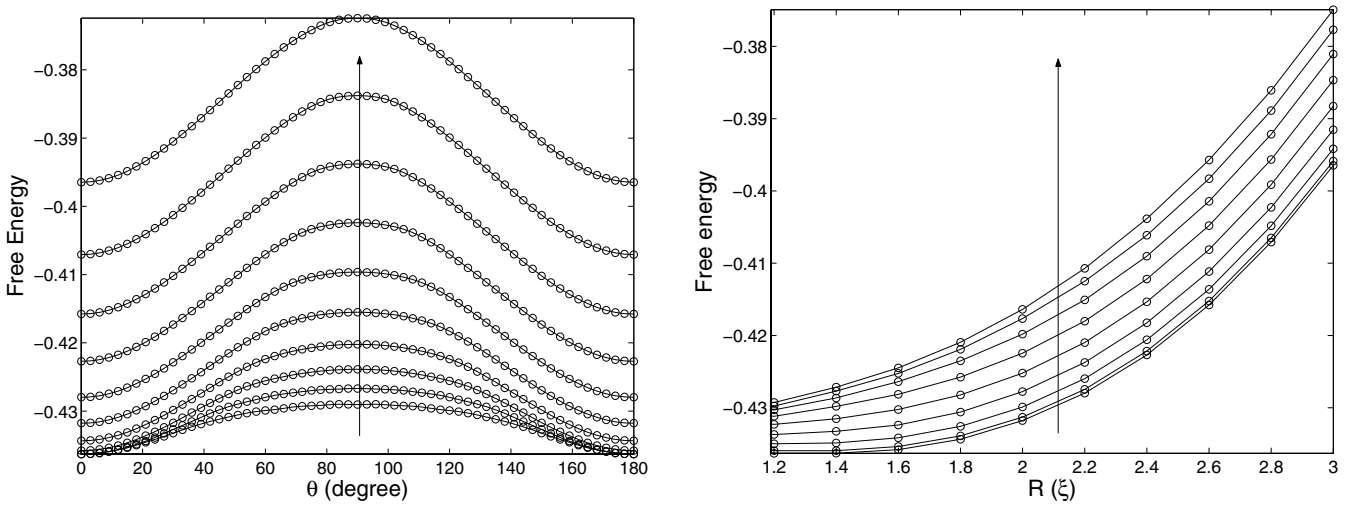


(a) (b)

**Fig. 3.** Dependency of the free energy, $\mathcal{F}$, with the pinning center radius $R$ and the angle $\theta$. (a) Variation of $\mathcal{F}$ as a function of the angle $\theta$ in the range 0° to 180°, data points obtained for increments of 3°. The radius $R$ varies from $1.2\xi$ to $3.0\xi$ and for each increment of $0.2\xi$ results in a distinct curve, all plotted in ascendant order as specified by the arrow. (b) Variation of $\mathcal{F}$ as a function of the pinning center radius for a specific value of $\theta$. The radius varies from $1.2\xi$ to $3.0\xi$ with a increment of $0.2\xi$. Distinct curve correspond to different $\theta$, equal to 0°, 9°, 18°, 27°, 36°, 45°, 54°, 63° and 72° in the ascendant order indicated by the arrow.

$R > \xi$. This extra volume, of the insulating region outside the vortex core, grows with the size of the spheres and, as previously discussed, makes the energy approach zero, that is, the normal state, because there is less superconducting volume in the unit cell. This behavior is seen in Figure 3a for any angle and not only for 0°. The free energy density, as calculated by equation (2), versus $\theta$ is shown in Figure 3b for several radii, ranging from $R = 1.2\xi$ to $R = 3.0\xi$, in steps of $0.2\xi$. It shows symmetry with respect to 90°, as expected, since the two zigzag paths, associated to $\theta$ and to $180° - \theta$, are just mirror images of each other, and so, have the same energy. For all radii, the configuration of minimum energy is for 0° and the maximum for 90°, because the 90° arrangement has a smaller fraction of superconducting volume as compared to the 0° configuration. For 0° the two spheres are aligned along the $z$-axis and both pin the vortex line whereas for 90° only one sphere pins the vortex and the other one is free in space, and so there is less condensate energy. This makes the superconductor closer in energy to the normal state, thus increasing its energy according to equation (2). At some intermediate angle between 0° and 90° occurs the depinning transition, although it is not noticeable in both Figures 3a and 3b. The depinning transition is not perceptible in $\mathcal{F}(\theta)$, nor in its derivative with respect to $\theta$, because of numerical limitations, possibly due to the coarseness of the mesh used in our calculations. In summary Figures 3a and 3b provide different views of the same data, which shows that the free energy density increases with $R$, a property previously explained in terms of the superposition of the vortex line with the pinning spheres.

The depinning transition is revealed by the kinetic energy of equation (3), though it steadily grows with $\theta$, reaching its maximum and minimum at the extremes 0° and 90°, respectively.

The depinning transition is best seen in the derivative $d\mathcal{F}_{kin}/d\theta$ versus $\theta$ curve. Figures 4a and 4b show the kinetic energy and its derivative for two selected radii, namely $R = 1.8\xi$, and $R = 2.4\xi$. Both cases show that the kinetic energy derivative vanishes for 0° and 90°, within numerical precision, which implies that the kinetic energy derivative must have at least one maximum in between these extreme angles [19]. Indeed these curves, as shown in Figures 4a and 4b, display a double hump structure with the lowest angle one as the absolute maximum. The depinning transition corresponds to the critical angle which defines the local minimum, located between the two humps. The critical angle defined by this procedure is listed in Table 1 for several radii. The reason for the second hump relies on the superposition of the vortex core with the two pinning centers. As long as it happens the order parameter has to adjust around one single common interface. However above the depinning transition, the vortex unpins from one of the spheres, yielding two independent surfaces where the deflection of the order parameter must take place. This leads to an extra growth of the kinetic energy above the transition because an order parameter gradient is set around two surfaces instead of just one.

The most relevant results of this paper are summarized in Figure 5, which shows the critical relative pinning length, as computed from equation (1) for several pinning sphere radii. The content of this figure is that of Table 1. The usefulness of plotting $\Delta l/l(\theta_c)$ instead of $\theta_c$ is to get direct information about the relative increase of the vortex line in presence of the zigzag arrangement of pinning centers. For instance, for the selected radii, $R = 1.8\xi$ and $R = 2.4\xi$, Figure 5 directly gives that the vortex line can

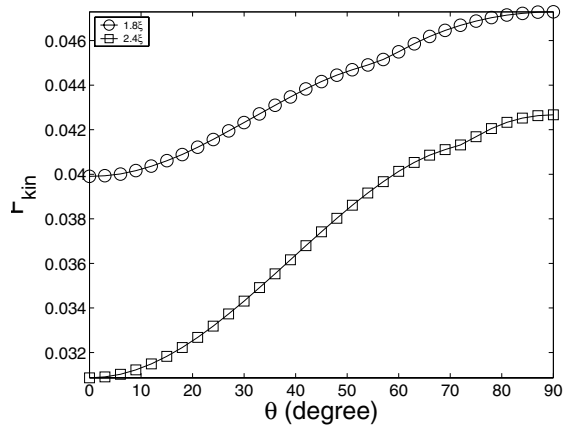


(a)

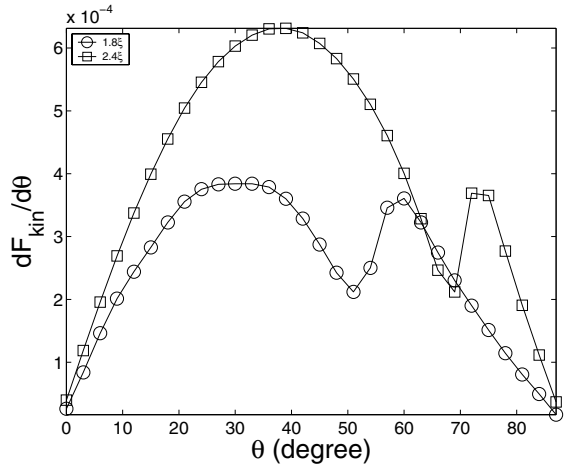


(b)

**Fig. 4.** The kinetic energy and its derivative. In (a) the curves $F_{kin} \times \theta$ for $R = 1.8\xi$ and $R = 2.4\xi$. In (b) their derivatives.

**Table 1.** The critical angle $\theta_c$ is given here, defined by the local minimum of the curves of Figures 4.

| Radius ($\xi$) | $\theta_c$(degree) |
|---|---|
| 1.2 | 33° |
| 1.4 | 42° |
| 1.6 | 48° |
| 1.8 | 54° |
| 2.0 | 60° |
| 2.2 | 66° |
| 2.4 | 72° |
| 2.6 | 75° |
| 2.8 | 78° |
| 3.0 | 81° |

stretch to a maximum of 31% and 46%, respectively, in presence of this zigzag of pinning centers. The strongest pinning corresponds to the maximum pinning sphere size, which is $R = 3.0\xi$. In this case the depinning transition occurs for $\theta_c = 81°$, and Figure 5 shows that this maximum vortex line stretch is 54%, thus below the maximum limit of $61,8\%$ reached for 90°, represented in Figure 5 through a dashed line.

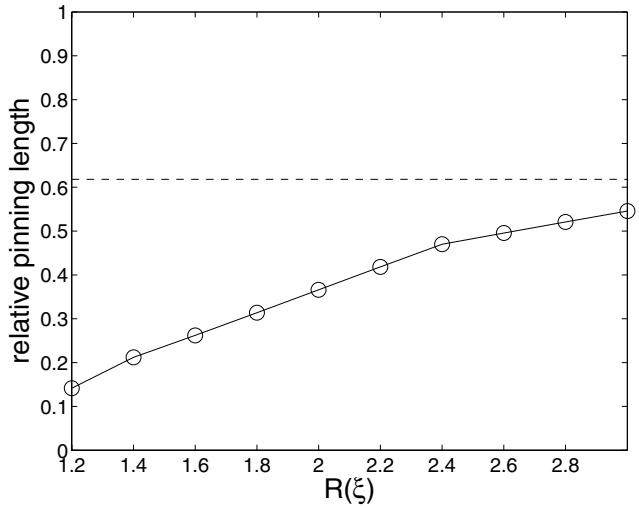


**Fig. 5.** Critical vortex line versus the radius of the pinning sphere. The dashed line means the maximum relative pinning length that is independent of the pinning center radius $R$.

The present results are best understood through Figures 6 and 7 which show semi-transparent views of the vortex and of the pinning sphere surfaces [20].

Figures 6a and 7a show that for $R > \xi$ the pinning sphere volume is partially outside the vortex core. As previously discussed this extra insulating volume costs energy causing the free energy of the superconductor to approach the normal state, which means to increase with $R$, as shown in Figure 3a. Figures 6 and 7 show three-dimensional plots of the normalized density $|\Delta|^2$ for radii $R = 1.8\xi$ and $R = 2.4\xi$, respectively, taken at angles 0°, 9°, 18°, 27°, 36°, 45°, 54°, 63°, and 72°. Each tridimensional figure shows an iso-surface of constant density inside the unit cell, taken here as a fraction of the maximum value of the normalized density, $|\Delta|^2_{iso} = (|3\Delta|^2_{max} + |\Delta|^2_{min})/4$. It also shows the pinning sphere surfaces and this provides a way to see in these plots the length scales of $1.8\xi$ and $2.4\xi$, respectively. Notice that above the depinning transition there is an iso-surface sphere, $|\Delta|^2_{iso}$, inside the pinning spheres. The order parameter does not drop abruptly to zero inside the pinning spheres because the functions $\tau_i$, taken in our calculations, are smooth versions of the Heaviside function, defined as $\tau = 1$ outside the spheres and $\tau = 0$ inside them. Abrupt changes within a distance smaller than two neighbor mesh points can lead to numerical instability, and for this reason some degree of smoothness is necessary because of our coarse-grain treatment of this problem. Figure 6 shows the behavior of the vortex line inside the unit cell for several angular arrangements of the two pinning spheres with $R = 1.8\xi$, ranging from Figure 6a until the depinning transition in Figure 6g. Pinning of the vortex by the top sphere becomes increasingly more difficult as $\theta$ increases resulting that Figures 6h and 6i describe configurations above the depinning transition. Figure 7 shows a similar sequence of angular arrangements with the depinning transition corresponding to Figure 7i. For both

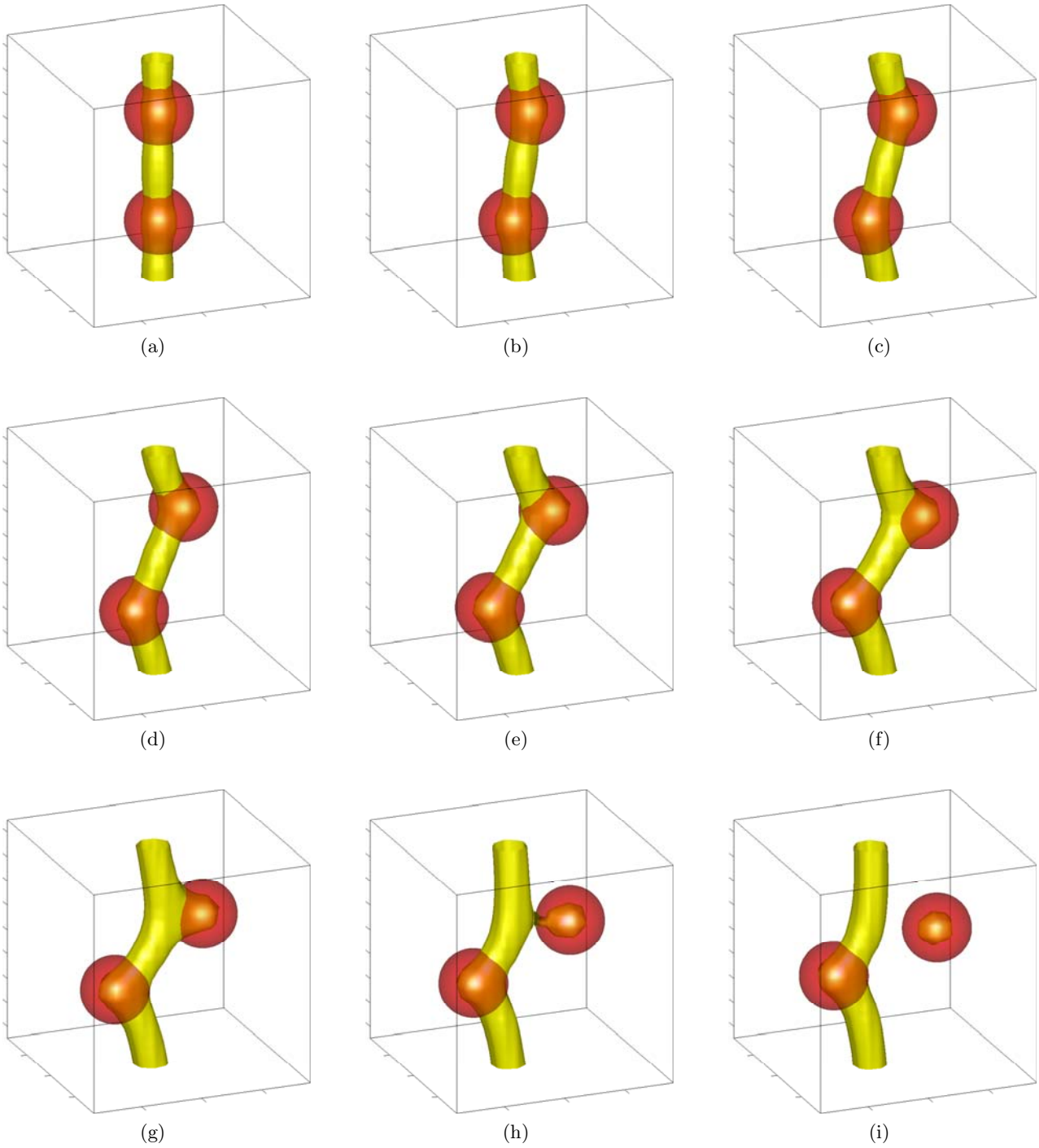


**Fig. 6.** Visualization of the order parameter density $|\Delta|^2$ and of the pinning centers of radius $R = 1.8\xi$. Extreme density values in the unit cell are $|\Delta|^2_{max} = 0,9990$ and $|\Delta|^2_{min} = 0,0034$. The density is visualized for $|\Delta|^2_{iso} = 0,2522$. The figures from 6a to 6i correspond to $\theta$ equal to 0°, 9°, 18°, 27°, 36°, 45°, 54°, 63° and 72° degree, respectively.

radii, as well as for any other one, we find that the depinning always occurs from the top sphere and never from the bottom one. This apparent breaking of symmetry is a consequence of the way the numerical procedure is carried here. All the sub-figures of Figure 6 were independently obtained from each other in our numerical simulations, and the same is true for the sub-figures of Figure 7. Each one of them results from an initial arbitrary configuration of the order parameter that evolves as the temperature of the Simulating Annealed method is lowered and the final configuration is reached within some convergence criteria. The reason for this breaking of symmetry is the way that the order parameter configuration is updated during the minimization procedure. The order parameter is updated

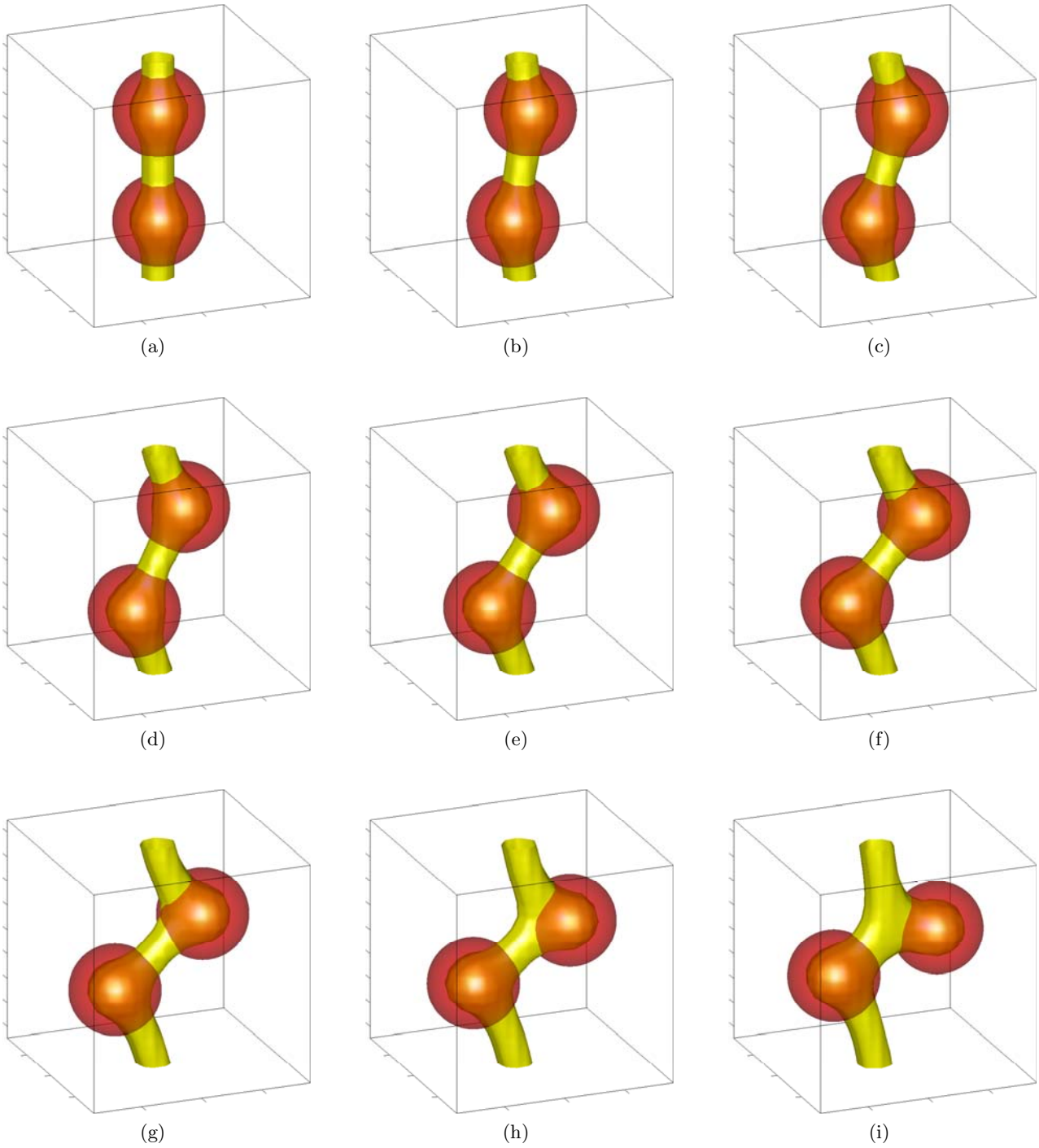


**Fig. 7.** Visualization of the order parameter density $|\Delta|^2$ and of the pinning centers of radius $R = 2.4\xi$. Extreme density values in the unit cell are $|\Delta|^2_{max} = 0,9990$ and $|\Delta|^2_{min} = 0,0035$. The density is visualized for $|\Delta|^2_{iso} = 0,2507$. The figures from 7a to 7i correspond to $\theta$ equal to 0°, 9°, 18°, 27°, 36°, 45°, 54°, 63° and 72° degree, respectively.

in sweeps of the mesh points of the unit cell that start from the bottom and end in the top. For this reason the vortex line remains pinned to the bottom sphere.

## 5 Conclusions

The length a vortex line inside a superconductor with pinning centers in case of no thermal fluctuations, is not just determined by the direction of the applied field and the geometry of the sample. The vortex line is subjected to the two conflictual demands of pinning by as many defects as possible, and its consequent increase in self-energy. We have studied here this problem in the context of a simple model with just one kind of pinning center, insulating spheres of coherence length size radius, forming a zigzag near the vortex line. The zigzags are periodically arranged

and form a lattice, which is simply described by a cubic unit cell with two pinning centers inside, whose center of the segment that connects them coincides with the center of the cube. This segment is free to rotate around its center producing for each angle a different zigzag path, whose pinning centers interact with the vortex line that pierces a pile of unit cell along the $z$-axis. The simplest possible zigzag arrangement is the straight line of insulating spheres of equal radii intercalated by two segments that pins the vortex line along the $z$-axis. As the pinning spheres inside the unit cell rotate a different zigzag of defects is produced, resulting for each rotation a vortex line more and more deviated from the straight line. The balance between the two competing effects, that is, defect trapping and self energy, changes with angle to the point that a depinning transition occurs and the vortex becomes nearly straight again. This maximum stretch of the vortex line depends on the pinning strength, here associated to the radius of the pinning sphere. We have numerically determined this depinning transition for a special pinning center lattice, with density, $2/L^3$, $L = 12.0\xi$, and several pinning strength, represented by radii, ranging from $R = 1.2\xi$ to $R = 3.0\xi$. We find that for this lattice the maximum length increase of the vortex line is 54% bigger than the straight line.

Research supported in part by Instituto do Milênio de Nano-Ciências, CNPq, and FAPERJ (Brazil).

## References


1. G.S. Mkrtchyan, V.V. Shmidt, Soviet Physics JETP **34**, 195 (1972)
2. E.H. Brandt, Rep. Prog. Phys. **58**, 1465 (1995)
3. J.B. Ketterson, S.N. Song, *Superconductivity*, 1st edn. (Cambridge University Press, 1999)
4. W.V. Pogosov, V.V. Moshchalkov, Physica C **404**, 285 (2004)
5. A.I. Buzdin, Phys. Rev. B **47**, 11416 (1993)
6. J.Y. Lin, M. Gurvitch, S.K. Tolpygo, A. Bourdillon, S.Y. Hou, J.M. Phillips, Phys. Rev. B **54**, R12717 (1996)
7. V.V. Moshchalkov, M. Baert, V.V. Metlusko, E. Rossell, M.J. Van Bael, K. Temst, Y. Bruynserade, Phys. Rev. B **57**, 3615 (1998)
8. V. Yurchenko, P. Lahl, S. Bunte, M. Jirsa, R. Wordenweber, Physica C **404**, 426 (2004)
9. A. Bezryadin, B. Pannetier, J. of Low Temp. Phys. **98**, 251 (1995)
10. W.H. Press, W.T. Vetterling, S.A. Teukolsky, B.P. Flannery, *Numerical Recipes*, 2nd edn. (Cambridge University Press, 1989)
11. A.A. Abrikosov, Soviet Physics JETP **5**, 1174 (1957)
12. A.I. Larkin, Sov. Phys.-JETP **31**, 784 (1970)
13. M.M. Doria, S.C.B. Andrade, Phys. Rev. B **60**, 13164 (1999)
14. M.M. Doria, G.F. Zebende, Brazilian J. Phys. **32**, 690 (2002)
15. M.M. Doria, G.F. Zebende, Phys. Rev. B **66**, 064519 (2002)
16. D.J. Priour, H.A. Fertig, Phys. Rev. B **67**, 054504 (2003)
17. P.G. de Gennes, *Superconductivity in Metals and Alloys*, 2nd edn. (Persus Book, 1989)
18. M.M. Doria, A.R. de C. Romaguera, Europhys. Lett. **67**, 446 (2004)
19. M.M. Doria, S. Salem-Sugui Jr, I.G. de Oliveira, L. Ghivelder, E.H. Brandt, Phys. Rev. B **65**, 144509 (2002)
20. A.R. de C. Romaguera, see animations in `http://www.if.ufrj.br/~ton`